Available online at www.sciencedirect.com
SCIENCE DIRECT®
Journal of Inorganic Biochemistry 98 (2004) 1067–1077
JOURNAL OF Inorganic Biochemistry
www.elsevier.com/locate/jinorgbio

# A model for the misfolded bis-His intermediate of cytochrome *c*: the 1–56 N-fragment

Elisa Santoni [a], Silvia Scatragli [a], Federica Sinibaldi [b], Laura Fiorucci [b], Roberto Santucci [b], Giulietta Smulevich [a,*]

[a] *Dipartimento di Chimica, Università di Firenze, Via della Lastruccia 3, I-50019 Sesto Fiorentino (FI), Italy*
[b] *Dipartimento di Medicina Sperimentale e Scienze Biochimiche, Università di Roma "Tor Vergata", V. Montpellier 1, 00133 Rome, Italy*

Received 14 November 2003; received in revised form 9 February 2004; accepted 19 February 2004
Available online 2 April 2004

**Abstract**

We have characterized the ferric and ferrous forms of the heme-containing (1–56 residues) N-fragment of horse heart cytochrome *c* (cyt *c*) at different pH values and low ionic strength by UV–visible absorption and resonance Raman (RR) scattering. The results are compared with native cyt *c* in the same experimental conditions as this may provide a deeper insight into the cyt *c* unfolding-folding process. Folding of cyt *c* leads to a state having the heme iron coordinated to a histidine (His18) and a methionine (Met80) as axial ligands. At neutral pH the N-fragment (which lacks Met80) shows absorption and RR spectra that are consistent with the presence of a bis-His low spin heme, like several non-native forms of the parental protein. In particular, the optical spectra are identical to those of cyt *c* in the presence of a high concentration of denaturants; this renders the N-fragment a suitable model to study the heme pocket microenvironment of the misfolded (His–His) intermediate formed during folding of cyt *c*. Acid pH affects the ligation state in both cyt *c* and the N-fragment. Data obtained as a function of pH allow a correlation between the structural properties in the heme pocket of the N-fragment and those of non-native forms of cyt *c*. The results underline that the (57–104 residues) segment under native-like conditions imparts structural stability to the protein by impeding solvent access into the heme pocket.


*Keywords:* Resonance Raman spectroscopy; Cytochrome *c* fragment; pH effect; Electronic absorption; Non-native form

## 1. Introduction

Cytochrome *c* (cyt *c*) has been extensively studied due to its important role as an electron transfer protein and is now well characterised both structurally (on the basis of spectroscopy and X-ray crystallography) and catalytically. Its folding kinetics have been followed spectroscopically; changes occurring in the heme pocket were monitored by electronic absorption (UV–Vis), circular dichroism (CD) [1,2] and resonance Raman (RR) techniques [3–8], whereas the changes in molecular size were followed by fluorescence emission of the single Trp residue as a function of denaturant concentration [4,9]. Unfolding of cyt *c* with chemical denaturants destabilizes the Met80 coordination, whereas the Fe–His18 bond remains intact under moderate unfolding conditions due to the nearby thioether linkages to the heme. At acid pH or in the presence of guanidine hydrochloride (GuHCl) or urea, cyt *c* undergoes various coordination and spin state changes. At pH 7.0 in the presence of denaturants the Met80 ligand is replaced by a misligated His (His33 or His26) giving rise to a misfolded intermediate characterized by a 6-coordinate (6c) low-spin (LS) form and a more relaxed heme compared to the wild-type protein. In a successive step, upon lowering the pH, one of the two His residues is replaced by a water molecule resulting in a 6c high-spin (HS) heme which coexists with a 5-coordinate (5c) HS species. These intermediates, which can be easily characterized via RR spectroscopy at equilibrium, have also been observed upon submillisecond folding of cyt *c* [3,5–8,10].

* Corresponding author. Tel.: +39-055-457-3083; fax: +39-055-457-3077.
*E-mail address:* giulietta.smulevich@unifi.it (G. Smulevich).

0162-0134/$ - see front matter © 2004 Elsevier Inc. All rights reserved.
doi:10.1016/j.jinorgbio.2004.02.026

The production of fragments of cyt *c*, obtained either by de novo synthesis or by enzymatic digestion of a native protein, offers the potential to extend and exploit this solid base of knowledge for cyt *c* to examine in detail simplified systems which may constitute good models of folding intermediates. Cyt *c* could be divided into a heme peptide of 65 residues and a non-heme peptide of 39 residues by treatment of the molecule with cyanogen bromide. Upon mixture of the two peptides in aqueous solution, a 1:1 complex with properties clearly resembling those of the parent enzyme was formed [11,12]. The earliest detectable intermediate on the folding pathway of cyt *c* could be mimicked by the complex formed by an N-terminal fragment (residues 1–38 with attached heme) and a C-terminal peptide [13]. As the fragment is unable to form this complex without the heme, the structural organization of the peptide fragments of cyt *c* triggered by heme binding has been also investigated [14]. Recently, the heme-containing 1–56 N-fragment (hereafter indicated as N-fragment) of cyt *c* has been obtained by limited proteolysis [15] of the parental protein and has been investigated by CD, UV–Vis and electronic paramagnetic resonance (EPR) at neutral pH [16]. The N-fragment contains the active site still covalently bound to a relatively large polypeptide chain, but lacks the C-terminal (residues 87–102) and the 60's (residues 60–69) α-helix segment, which forms the native hydrophobic core with the N-terminal helix (residues 6–14) and the heme group. Furthermore, the Met80 axial ligand of the native enzyme is absent in the N-fragment. The results indicated that the N-fragment shows a compact structure, but lacks an ordered secondary structure. The heme group is suggested to be axially bound to two His residues and is shielded from solvent by the peptide chain. Furthermore, cyt *c* reconstituted from the N-fragment and the C-fragment (residues 57–104) displays native-like redox properties [17].

In the present work, we extend further the characterization of the N-fragment using both electronic absorption and RR spectroscopy at various pH values and at low ionic strength. Experiments on the N-fragment and native cyt *c* have been carried out in parallel under the same experimental conditions enabling us to conclude that at pH 7.0 the ferric N-fragment has a bis-His LS heme, as found for the misfolded His–His intermediate that forms during folding of cyt *c*. Furthermore, pH-dependent titrations of cyt *c* and the N-fragment show a different protonation profile resulting from either the different heme iron axial ligands or from the shielding effect of the polypeptide chains. Finally, the spectra of the ferrous form at various pH values markedly differ from the corresponding spectra of the native protein, since around neutral pH one of the two His is protonated giving rise to a 5cHS species characterized by a fairly strong Fe–Im bond coexisting with a bis-His LS species.

## 2. Materials and methods

Horse heart cyt *c* (type IV) was purchased from Sigma and used without further purification. The N-fragment was obtained as previously reported [16].

The protein samples were prepared in 10 mM sodium phosphate at pH 7.0. Lower pH values were obtained by adding 500 mM HCl to the pH 7.0 protein solution: the maximum concentration of HCl in the solution was about 60 mM, at pH 1.3. The pH of the samples was measured before and after the RR measurements.

A very small amount of potassium hexacyanoferrate (III) was added to the solution of the Fe(III) cyt *c* samples to ensure that the protein was completely oxidised.

Table 1
RR spectral parameters of the $\nu_3$ mode of cyt *c* and N-fragment at different pH values obtained by a band fitting program using Lorentzian line shapes

| | 6cLS | | 6cHS | | 5cHS | |
|---|---|---|---|---|---|---|
| | 6cLS(1) | 6cLS(2) | 6cHS(1) | 6cHS(2) | 5cHS(1) | 5cHS(2) |
| | His–Fe–Met80 | His–Fe–His18 | His–Fe–$H_2O$ | $H_2O$–Fe–$H_2O$ | His–Fe | $H_2O$–Fe |
| *N-fragment* | | | | | | |
| pH 7.0 | | 1505 (100) [15] | | | | |
| pH 3.8 | | 1506 (60) [15] | 1483 (33) [18][a] | | 1495 (7) [13] | |
| pH 3.0 | | 1506 (27) [15] | 1483 (55) [18][a] | | 1495 (6) [13] | 1492 (12) [13] |
| pH 2.0 | | 1506 (4) [15] | | 1483 (48) [14] | | 1492 (48) [13] |
| *Cyt c* | | | | | | |
| pH 7.0 | 1502 (100) [11] | | | | | |
| pH 2.5 | 1502 (32) [11] | 1505 (31) [15] | 1483 (37) [18][a] | | | |
| pH 2.3 | 1502 (9) [11] | 1505 (24) [15] | | 1483 (38) [14] | | 1492 (29) [13] |
| pH 1.3 | 1502 (6) [11] | 1505 (12) [15] | | 1483 (38) [13] | | 1492 (44) [13] |

Frequencies are given in $cm^{-1}$; band intensities (in parentheses) are expressed as percentages; bandwidths (in square brackets) are given in $cm^{-1}$.
[a] The large bandwidth suggests that the $\nu_3$ bands of two 6cHS species overlap (see text).

The ferrous forms were obtained by a 5% volume addition of a fresh sodium dithionite (20 mg/ml) solution to a deoxygenated protein solution. The following buffers were used: 0.1 M sodium citrate at pH 5.5, 0.1 M sodium phosphate at pH 7.0 and 0.1 M borate at pH 9.0.

Sample concentration was about 0.03–0.06 mM for RR spectroscopy and about 0.05–0.1 mM for UV–Vis absorption.

Absorption spectra, recorded with a Cary 5 spectrophotometer, were measured both prior to and after RR measurements. No degradation was observed under the experimental conditions used. The RR spectra were obtained by excitation with the 406.7 and 413.1 nm lines of a $Kr^+$ laser (Coherent, Innova 302) and with the 441.6 nm line of a He–Cd laser (Kimmon IK4121R-G). The backscattered light from a slowly rotating NMR tube was collected and focused into a computer-controlled double monochromator (Jobin-Yvon HG 2S 2000) equipped with a cooled photomultiplier (RCA C31034A) and photon counting electronics. The RR spectra were calibrated with indene and $CCl_4$ as standards to an accuracy of $\pm 1$ $cm^{-1}$ for isolated bands. In the figures the relative intensities of the high-frequency RR bands are normalized on the $\nu_4$ band (not shown in the figures).

Peak intensities and positions of the $\nu_3$ RR bands of the cyt *c* N-fragment at different pH values were determined by a curve-fitting program (Table 1).

All the electronic absorption and RR spectra were collected at about 20–25 °C.

## 3. Results and discussion

### 3.1. Ferric form

#### 3.1.1. Electronic absorption

Fig. 1 shows the electronic absorption spectra of ferric cyt *c* (Fig. 1(A)) and the N-fragment (Fig. 1(B)) at various pH values. The UV–Vis spectrum of native cyt *c* at pH 7.0 displays the characteristic Soret band at 409 nm, Q bands at about 560 and 530 nm, and a weak charge-transfer (CT) band at 695 nm, indicative of a 6cLS heme with His (His18) and Met (Met80) residues bound to the iron atom. As the heme pocket structure is sensitive to the ionic strength at acid pH [18], the measurements carried out upon lowering the pH were made in conditions of low ionic strength (4.6 mM $Cl^-$). The 695 nm absorption band of the native 6cLS protein starts decreasing at pH 3.8 and, at pH 3.5, its decrease is clearly accompanied by the appearance of a new band at 620 nm. This band further increases in intensity (at the expense of the band at 695 nm) upon decrease of pH with a concomitant blue-shift of the Soret band (to 395 at pH 2.3 and to 394 at pH 1.3) and the appearance of a new band in the Q region at 495 nm. In agreement with previous reports, these changes are considered to result from the decrease of the 6cLS species, due to the rupture of the Fe–Met80 bond, and the formation of HS species [18].

At pH 7.0 the N-fragment is characterized by a 6cLS heme giving rise to an electronic absorption spectrum maxima at 406, 528 and 557 nm (Fig. 1(B)), blue-shifted compared to cyt *c*. Moreover, the CT band at 695 nm is absent since the native Met80 axial ligand is missing. Unlike the native protein, ionic strength does not influence the protonation of the ligands. According to the p$K_a$ of 4.15, obtained by pH titration curves, a CT1 at 620 nm appears at pH 5.2 and becomes clearly evident at pH 4.8. Further decrease of pH causes changes which are similar to those observed for cyt *c* and characterized by a blue shift of the Soret band to 394 nm at pH 2.0, an intensity decrease of the Q-bands of the LS heme and the appearance of the Q-band typical of HS species. No further changes are observed at pH lower than 2.0. Moreover, unlike cyt *c*, the absorption spectra of the N-fragment show two isosbestic points at 403 and 585 nm between pH 7.0 and 3.8 (data not shown), indicating the conversion from one form to another.

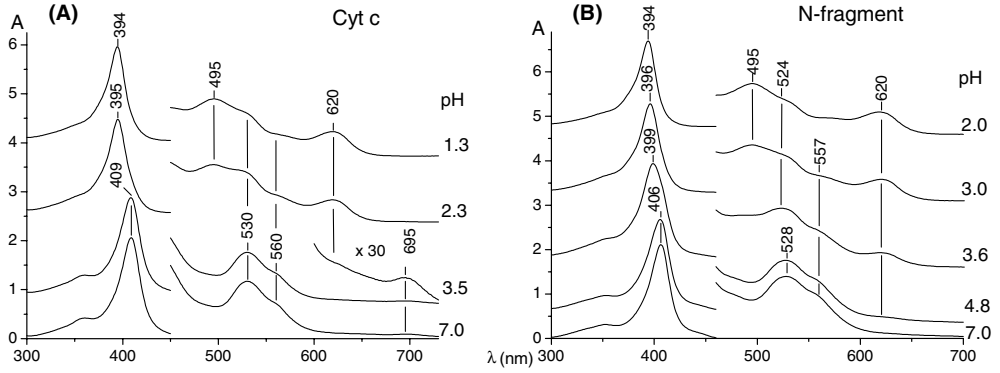


Fig. 1. Electronic absorption spectra of oxidized cyt *c* (panel A) and the N-fragment (panel B) at different pH values. Panel A: from bottom to top, pH 7.0, 3.5, 2.3, 1.3. Panel B: from bottom to top, pH 7.0, 4.8, 3.6, 3.0, 2.0. The visible region has been expanded 6-fold in both panels A and B except for the spectrum at pH 3.5 (panel A) that has been expanded 30-fold.

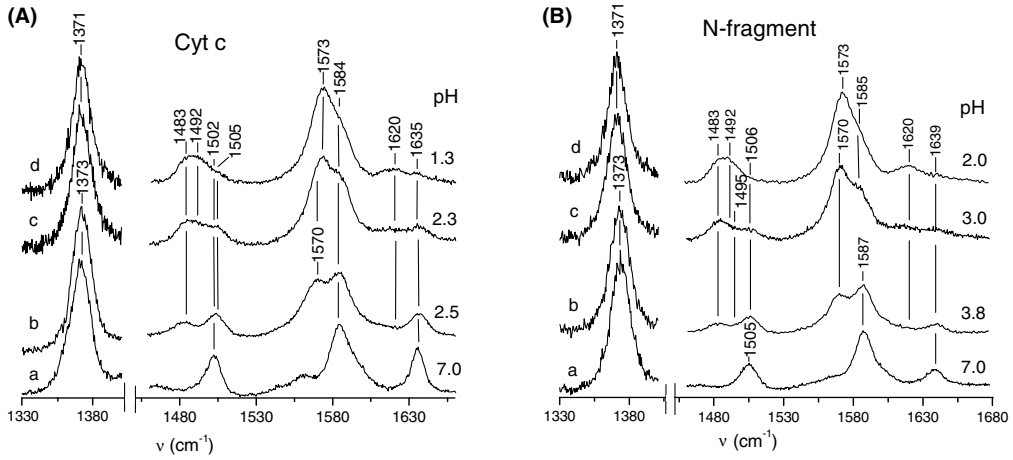


Fig. 2. Resonance Raman spectra of oxidized cyt *c* (panel A) and the N-fragment (panel B) at different pH values. Panel A: (a) pH 7.0, (b) pH 2.5, (c) pH 2.3, (d) pH 1.3. Panel B: (a) pH 7.0, (b) pH 3.8, (c) pH 3.0, (d) pH 2.0. RR experimental conditions: 406.7 nm excitation wavelength; 5 $cm^{-1}$ resolution. For $\nu_4$ spectra region (1330–1405 $cm^{-1}$) the collection interval is 1 s/0.5 $cm^{-1}$. Panel A: (a) 20 mW laser power at the sample, 6 s/0.5 $cm^{-1}$ collection interval; (b) 20 mW, 7 s/0.5 $cm^{-1}$ collection interval. (c) 10 mW, 18 s/0.5 $cm^{-1}$ collection interval; (d) 10 mW, 19 s/0.5 $cm^{-1}$ collection interval. Panel B: 20 mW laser power at the sample, (a) 22 s/0.5 $cm^{-1}$ collection interval; (b) 22 s/0.5 $cm^{-1}$ collection interval; (c) 11 s/0.5 $cm^{-1}$ collection interval; (d) 12 s/0.5 $cm^{-1}$ collection interval.

*3.1.2. Resonance Raman spectroscopy*

RR spectra confirm the conversion from LS to HS species at acid pH for both the native protein and the N-fragment (Fig. 2). At neutral pH the RR spectra of cyt *c* are extremely rich, especially in the low-frequency region [19] due to the heme–protein interactions which result in a pronounced saddling distortion of the heme group in the native structure [20]. Nevertheless, its RR bands were completely assigned [21]. The core size marker bands in the high frequency region (Fig. 2(A)) are at 1502 $cm^{-1}$ ($\nu_3$), 1584 $cm^{-1}$ ($\nu_2$), and 1635 $cm^{-1}$ ($\nu_{10}$). The pronounced saddling distortion of the heme group in the native structure [20] is manifested in the RR spectra by the lower frequencies of the core size marker bands compared to planar heme proteins, which display an inverse correlation between the RR band frequencies and the metalloporphyrin core size [22–25]. At pH 2.5 a net decrease of the intensity of the core size marker bands of the 6cLS heme is observed with the appearance of new bands at 1483, 1570 and 1620 $cm^{-1}$ corresponding to a 6cHS species. At pH 2.3 this tendency is more pronounced and the amount of the HS species is higher than the LS form. Moreover, in the $\nu_3$ region the band broadens and the frequency of the $\nu_3$ marker band of the 6cLS species is slightly higher than that of the native form. Upon further lowering of the pH (pH 1.3) the 6cLS heme is largely reduced and the bands of the HS species change shape and shift to higher frequency indicating the formation of a new species.

In order to obtain information on the species formed during acid denaturation we have analyzed the components of the RR spectra by curve fitting of the $\nu_3$ region (Fig. 3(A), Table 1). In the first step, the minimum number of contributing species and their approximate component spectra have been determined. Subsequently, the initial spectra are iteratively refined in a global fit to all measured spectra.

Acid pH induces the formation of at least three new species corresponding to the bands at 1505 $cm^{-1}$ [6cLS(2)], 1483 $cm^{-1}$ [6cHS], and 1492 $cm^{-1}$ [5cHS(2)], whereas the native 6cLS(1) form characterized by the $\nu_3$ at 1502 $cm^{-1}$ decreases in intensity. Interestingly, at pH 2.5 the band at 1483 $cm^{-1}$ appears very broad (bandwidth 18 $cm^{-1}$), suggesting the coexistence of two 6cHS species, denoted as [6cHS(1)] and [6cHS(2)]. In analogy with previous work, at this pH, the 6cHS forms are assigned to a His18–Fe–$H_2O$ and $H_2O$–Fe–$H_2O$ ligated heme, respectively [7,10,18]. The new low spin species [6cLS(2)] corresponds to a non-native species of cyt *c*, previously observed in the range pH 2.5–0.5 at high ionic strength, but virtually absent at low ionic strength [18], and in the presence of sodium dodecyl sulfate (SDS), GuHCl, and urea. It is assigned to a misligated His18/His33 or His18/His26 heme [18,26]. The upshift of the core size marker bands compared to the native form is due to a partial relaxation of the heme distortion toward a more planar heme following the rupture of the Fe–Met80 bond and subsequent binding of a His residue. At pH 2.3 a 5cHS species at the expense of the LS forms appears and becomes more intense at lower pH (pH 1.3).

Therefore, this 5cHS species is assigned to a configuration in which a water molecule is axially bound to the heme iron [5cHS(2)] [27] following the protonation of the His18 ligand. Accordingly, the 6cHS form present at pH 1.3 and characterized by a narrow bandwidth of 13 $cm^{-1}$ is assigned to a bis-aquo coordinated heme [6cHS(2)]. The formation of an aquo-coordinated spe-

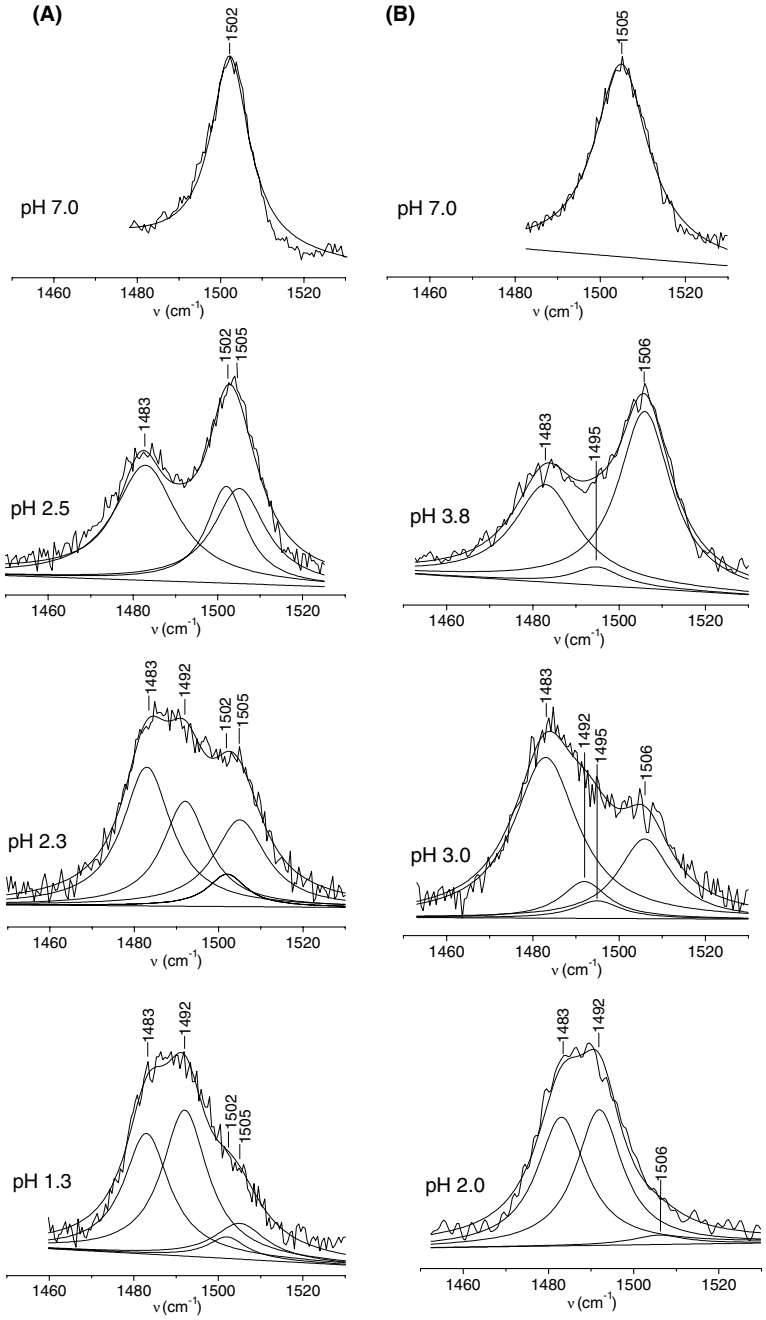


Fig. 3. Curve-fitting of the $\nu_3$ band of cyt c (Panel A) and N-fragment (Panel B) at the indicated pH values. The curve-fitting parameters are reported in Table 1.

cies is also supported by the relatively high $\nu_2/\nu_4$ intensity ratio (Fig. 2) in agreement with previous results [18].

The RR spectrum of the N-fragment at pH 7.0 (Fig. 2(B)) is typical of a 6cLS heme with core size marker bands at 1505 $cm^{-1}$ ($\nu_3$), 1587 $cm^{-1}$ ($\nu_2$), and 1639 $cm^{-1}$ ($\nu_{10}$). These frequencies, higher than those of the native cyt *c*, resemble those of the 6cLS observed for non native cyt *c* in the presence of denaturants or at acid pH [18] and are almost identical to those previously observed for the bis-His cytochrome *c″* [8]. In analogy with the non native LS form of cyt *c*, this species is identified as [6cLS(2)]. Characteristic HS bands [1483 $cm^{-1}$ ($\nu_3$), 1570 $cm^{-1}$ ($\nu_2$) and 1620 $cm^{-1}$ ($\nu_{10}$)] appear at pH 3.8 (Fig. 2(B)) and the spectrum closely resembles that observed for cyt *c* at pH 2.5. At pH 3.0 the 6cHS is the predominant form and the presence of a new HS species is suggested by the weak band at 1495 $cm^{-1}$. Further decrease of the pH to 2.0 clearly shows the almost complete disappearance of the 6cLS heme. Moreover, a broadening and the shift towards higher frequency (1492 $cm^{-1}$) of the $\nu_3$ band suggests the

formation of at least one more additional species besides the 6cHS form. A band-fitting analysis of the RR spectra in the $\nu_3$ region (Fig. 3(B) and Table 1) shows that a $\nu_3$ at 1495 $cm^{-1}$ is present at pH 3.8, decreases at pH 3.0 and disappears at pH 2.0. Concomitantly at pH 3.0 a new band at 1492 $cm^{-1}$ appears which becomes very strong at pH 2.0. The 5cHS present at higher pH is assigned to a His18 ligated form, deriving from the protonation of the first His residue [5cHS(1)]. The 5cHS species dominating at low pH is assigned to a mono-aquo form, as a consequence of the protonation of the second His ligand [5cHS(2)]. On the basis of these results, the 6cHS species at pH 3.8, characterized by a broad band at 1483 $cm^{-1}$ (bandwidth 18 $cm^{-1}$) is due to the overlap of a His–Fe–$H_2O$ [6cHS(1)] and a $H_2O$–Fe–$H_2O$ [6cHS(2)] form, the latter becoming the predominant form at pH 2.0. Therefore, we can conclude that protonation of the first His ligand at acid pH allows the coordination of a water molecule to the heme iron of the N-fragment and only a small amount of the 5c His–Fe configuration is present.

Further information can be obtained by the analysis of the low frequency RR region (Fig. 4). At neutral pH cyt *c* is characterized by a very complex spectrum (spectrum a, Fig. 4), since the peripheral substituent and the out-of-plane modes become active as a consequence of a fairly distorted heme [28]. In the N-fragment spectrum at pH 7.0 (spectrum b, Fig. 4) several bands can be seen to have a much lower intensity and frequency compared to cyt *c*. In particular, the bands assigned in cyt *c* to the out-of-plane modes $\gamma_{22}$ (447 $cm^{-1}$), $\gamma_{12}$ (521 $cm^{-1}$), $\gamma_{21}$ (567 $cm^{-1}$), and $\gamma_5$ (730 $cm^{-1}$) and the vibrations of the thioether linkage at 397 $cm^{-1}$ [$\delta(C_\beta C_a S)$]

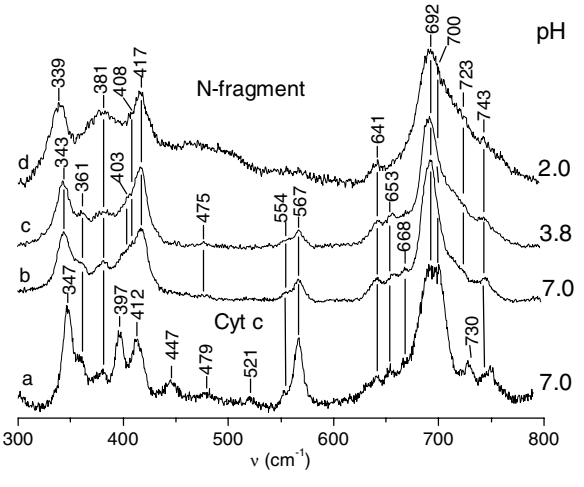


Fig. 4. Resonance Raman spectra of oxidized cyt *c* at pH 7.0 (a) and the N-fragment at pH 7.0 (b), pH 3.8 (c), pH 2.0 (d). RR experimental conditions: 406.7 nm excitation wavelength; 5 $cm^{-1}$ resolution. (a) 15 mW laser power at the sample, 3 s/0.5 $cm^{-1}$ collection interval; (b) 20 mW, 8 s/0.5 $cm^{-1}$ collection interval; (c) 20 mW, 10 s/0.5 $cm^{-1}$ collection interval; (d) 13 mW, 8 s/0.5 $cm^{-1}$ collection interval.

dramatically decrease in intensity. As observed for the high frequency region, the spectrum resembles very closely that of cyt *c″* [8] and in common with this latter protein it also shows the presence of a new band at 403 $cm^{-1}$ which is assigned to the bis-His asymmetric stretching mode [$\nu_{as}$(Fe–$Im_2$)], predicted to be Raman-active if the ligands are inequivalent [29]. Lowering the pH to 3.8 (spectrum c, Fig. 4) causes only slight changes in the spectrum which, on the other hand, changes dramatically at pH 2.0 (spectrum d, Fig. 4). The spectrum is almost identical to that of cyt *c* at pH 1.3 (data not shown) and to that of the protein unfolded in the presence of denaturants at acid pH [30]. Only a few bands are present, as all the out-of-plane modes and the bis-His asymmetric stretching mode [$\nu_{as}$(Fe–$Im_2$)] have disappeared. The assignment of the low-frequency RR bands of the N-fragment, based on the assignment of the bands of cyt *c*, is reported in Table 2.

### 3.2. Ferrous form

Fig. 5 shows the titration of the reduced N-fragment between pH 9.0 and 5.5. Unlike cyt *c*, which has a 6cLS heme in the range under investigation [27], on going from alkaline to acid pH the N-fragment undergoes coordination and spin state changes as a consequence of the protonation of one of the two His ligands. At alkaline pH the N-fragment is mainly 6cLS with maxima at 417, 520, and 550 nm. Interestingly, the Soret maximum is different from that observed for cyt *c* at neutral pH (415 nm) but identical to those observed for bis-His cytochromes such as cytochrome $c_3$ [31]. Moreover, as previously observed for the ferric form of cyt *c*, the peak maxima of the electronic absorption spectrum of the N-fragment resemble very closely those of cyt *c* on addition of GuHCl [32]. Upon lowering the pH a 5cHS grows at the expense of the 6cLS, as judged by the appearance of shoulders at 433 and 565 nm.

Fig. 6 compares the RR spectra obtained for the ferrous N-fragment in the high (panel A) and low (panel B) frequency region at pH 9.0 and 7.0. Experiments at pH 5.5 were not successful due to the instability of the reduced form in the laser beam. The experiments were carried out with excitations at 413.1 and 441.6 nm, where the LS and HS forms, respectively, are selectively resonance enhanced. Inspection of the spectra in the high frequency region (Fig. 6(A)) confirms the presence of an almost pure LS heme at alkaline pH. It is different from the corresponding spectrum of native cyt *c* [21] and is characterized by the intense bands at 1492 $cm^{-1}$ ($\nu_3$), 1535 $cm^{-1}$ ($\nu_{11}$), and 1591 $cm^{-1}$ ($\nu_2$). At pH 7.0 an increase of the 5cHS species (1469 $cm^{-1}$, $\nu_3$; 1546 $cm^{-1}$, $\nu_{11}$; 1572 $cm^{-1}$, $\nu_2$; and 1605 $cm^{-1}$, $\nu_{10}$) at the expense of the LS heme can be observed. Interestingly, addition of up to 1.6 mM SDS to neutral cyt *c* largely converts the native LS heme to a 5cHS form, which is converted to a

Table 2
RR bands ($cm^{-1}$) and mode assignments observed in the low frequency region for ferric and ferrous cyt *c* and N-fragment at pH 7.0 and 2.0

| Assignment | | Cyt *c*[a] | | N-fragment | | |
|---|---|---|---|---|---|---|
| | | pH 7.0 | | pH 7.0 | | pH 2.0 |
| | | $Fe^{2+}$ | $Fe^{3+}$ | $Fe^{2+}$ | $Fe^{3+}$ | $Fe^{3+}$ |
| $\nu_{34}$ $\delta(C_\delta C_1)_{sym}$ | $B_{2g}$ | 183 | | 190 HS; 199 LS | | |
| $\nu_{53}$ $\delta$(pyr transl) | $E_u$ | 202 | | 209 | | |
| $\gamma_{24}$ $\gamma(C_\alpha C_m)$ | $E_g$ | | 226 | | | |
| $\nu$(Fe–Im) | | | | 229 HS | | |
| | | 240 | | 238 LS | | |
| $\nu_9$ $\nu$(pyr) + $\delta$(substituents pyr) | $A_{1g}$ | 271 | 272 | 267 | | |
| $\nu_{51}$ $\delta(C_\beta C_1)_{asym}$ | $E_u$ | 309 | 304 | 309 | | |
| $\nu_8$ $\nu$(pyr) + $\delta$(substituents pyr) | $A_{1g}$ | 347 | 349 | 344 | 343 | 339 |
| $\nu_{50}$ $\nu$(pyr) + $\delta$(substituents pyr) | $E_u$ | 360 | 369 | 358 | 361 | |
| $\delta(C_\beta C_c C_d)$ | | 372, 382 | 380 | 377 | 381 | 381 |
| $\delta(C_\beta C_a S)$ | | 394, 401 | 397 | 400 LS | | |
| $\nu_{as}(Fe–Im_2)$ | | | | | 403 | |
| $\delta(C_\beta C_a C_b)$ | | 413, 421 | 412, 418 | 413 | 408, 417 | 408, 417 |
| $\gamma_{22}$ pyr swivel | $E_g$ | 442 | 442 | | | |
| $\nu_{33}$ $\delta$(pyr rotat) | $B_{2g}$ | 479 | 480 | | 475 | |
| $\gamma_{12}$ pyr swivel | $B_{1u}$ | 520 | 522 | | | |
| $\nu_{49}$ $\delta$(pyr rotat) | $E_u$ | 536 | | | | |
| $\gamma_{21}$ pyr $fold_{sym}$ | $E_g$ | 552, 568 | 567 | | 554, 567 | |
| $\nu_{48}$ $\delta(pyr\ deform)_{sym}$ | $E_u$ | 633, 642 | 632, 642 | | 641 | 641 |
| $\gamma_{20}$ pyr $fold_{asym}$ | $E_g$ | 653, 666 | 655, 666 | | 653, 668 | |
| $\nu(C_a S)$ | | 682, 692 | 693 | | 692 | 692 |
| $\nu_7$ $\delta(pyr\ deform)_{sym}$ | $A_{1g}$ | 700 | 701 | | 700 | 700 |
| $\gamma_{11}$ pyr $fold_{asym}$ | $B_{1u}$ | 724 | | | 723 | 723 |
| $\gamma_5$ pyr $fold_{sym}$ | $A_{2u}$ | 729 | 729 | | | |
| $\nu_{15}$ $\delta$(pyr breathing) | $B_{1g}$ | 750 | 750 | | 743 | 743 |

[a] From [21]. The following experimental conditions differ from those reported herein: temperature 12 K, excitation wavelength 413.1 nm; 50 mM potassium phosphate buffer with 0.5 M KCl added. Consequently, some of the cyt *c* frequencies of the spectra observed in Figs. 4 and 7 are slightly different.

6cLS heme upon addition of imidazole. As expected, the RR spectrum of the low spin heme of the N-fragment, closely resembles that of the imidazole complex of ferrous cyt *c* in SDS solutions [18].

Moreover, the same 6cLS species is observed also at pH 5.8 upon addition of 10 mM GuHCl to ferrous cyt *c* [18], whereas at higher concentration a 5cHS heme is already observed at neutral pH [33]. Fig. 6(B) compares the RR spectra of the N-fragment in the low frequency region. The low frequency region RR spectra of 5c ferrous hemoproteins are characterized by the presence of a strong band due to the iron–imidazole stretching mode, $\nu$(Fe–Im), which occurs in the region 200–250 $cm^{-1}$. As the spectra in the high frequency region, the spectra obtained with both the 441.6 and 413.1 nm excitation wavelength are quite different from those reported for the native cyt *c* at neutral pH ([21] and Table 2). At pH 7.0 a fairly intense band at 229 $cm^{-1}$ (which is not present in the RR spectrum of the native cyt *c*) is observed in the spectrum obtained with the 441.6 nm excitation wavelength (Fig. 6, a′). It is assigned to the $\nu$(Fe–Im) stretching mode since it is expected to be enhanced only in the 5cHS species. Confirmation that the band results from a Fe–Im stretching mode can be

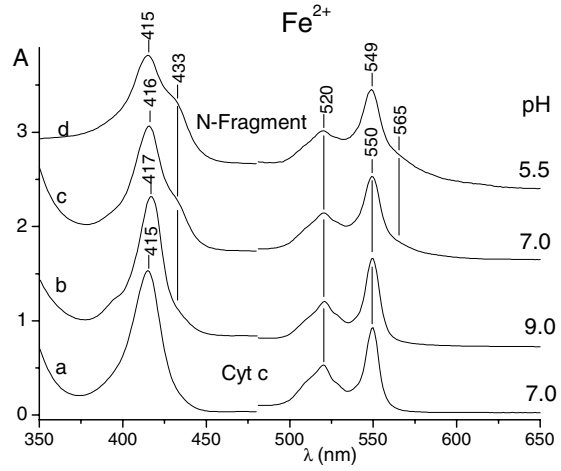


Fig. 5. Electronic absorption spectra of reduced cyt *c* at pH 7.0 (a) and the N-fragment at pH 9.0 (b), pH 7.0 (c) and pH 5.5 (d). The 470–650 nm has been expanded 5-fold (a, b, c) and 15-fold (d).

derived from the intensity decrease observed for excitation at 413.1 nm. This wavelength is out of resonance for the HS heme species (Soret maximum at 433 nm) and, hence, the Fe–Im stretching mode which is strongly coupled to the Soret resonance [29] is considerably weakened. It can be seen that the band at 229 $cm^{-1}$ is clearly weakened at pH 7.0 for this excitation wavelength and is nearly absent at pH 9.0.

The frequency of the *v*(Fe–Im) stretching mode is sensitive to the bond strength as a consequence of the status of the proton on the bound imidazole. A non H-bonded ligand has a frequency at about 200 $cm^{-1}$. As the strength of the hydrogen bond between the imidazole proton and an accepting residue increases, the observed *v*(Fe–Im) frequency also increases [34,35]. A frequency at 229 $cm^{-1}$ is fairly high and is reminiscent of the frequencies observed for the heme containing peroxidase enzymes for which a strong H-bond between the $N_\delta H$ proton of the imidazole and an Asp residue has been found [36]. It is very likely that the His bound to the iron is the native His18. On the basis of the X-ray structure of cyt *c* [20] a good candidate able to form such a H-bond with the His18 is Pro30, whose side chain carbonyl oxygen atom is located at 2.7 Å from the $N_\delta$ of the imidazole (Fig. 7). However, the value of the N-fragment *v*(Fe–Im) frequency is higher than those characteristic of systems in which the acceptors are side chain carbonyl oxygen atoms. Thus, it cannot be ruled out that other H-bond acceptor residues are in the vicinity of the His18 residue in the N-fragment when His33 or His26 are bound to the other coordination position of the heme. Nevertheless, the high frequency of the *v*(Fe–Im) stretching mode, which corresponds to a fairly strong Fe–Im bond, agrees very well with the finding that for ferrous cyt *c* there is no indication that the Fe–His18 bond is ruptured even in GuHCl (at pH > 3) [18]. As a consequence, a strong coordinative Fe–Im bond persists even in the absence of an appropriate protein fold in its immediate environment.

### 3.3. Role of the 57–104 peptide fragment

Table 3 summarizes the coordination-spin state changes observed for both native cyt *c* and the N-fragment upon lowering the pH. The titration of the ferric form at low ionic strength has revealed that although the protonation of the ligands in the two systems has a similar behaviour it occurs at different pH, being about one unit higher in the fragment than in the mother protein. This clearly depends on the different nature of

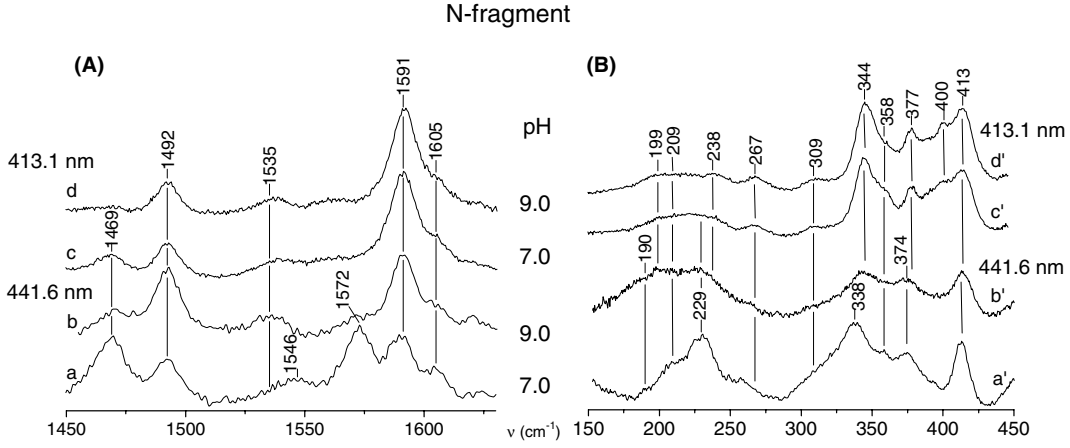


Fig. 6. Resonance Raman spectra of the reduced N-fragment at pH 7.0 (a, a′, c, c′) and 9.0 (b, b′, d, d′). RR experimental conditions: 5 $cm^{-1}$ resolution; 441.6 nm excitation wavelength ( a, a′, b, b′), 413.1 nm excitation wavelength (c, c′, d, d′); (a) 20 mW at the sample, 8 s/0.5 $cm^{-1}$ collection interval; (b) 15 mW at the sample, 14 s/0.5 $cm^{-1}$ collection interval; (c) 15 mW at the sample, 7 s/0.5 $cm^{-1}$ collection interval; (d) 15 mW at the sample, 8 s/0.5 $cm^{-1}$ collection interval; (a′) 20 mW at the sample, 8 s/0.5 $cm^{-1}$ collection interval; (b′) 20 mW at the sample, 32 s/0.5 $cm^{-1}$ collection interval; (c′) 15 mW at the sample, 9 s/0.5 $cm^{-1}$ collection interval; (d′) 15 mW at the sample, 4 s/0.5 $cm^{-1}$ collection interval.

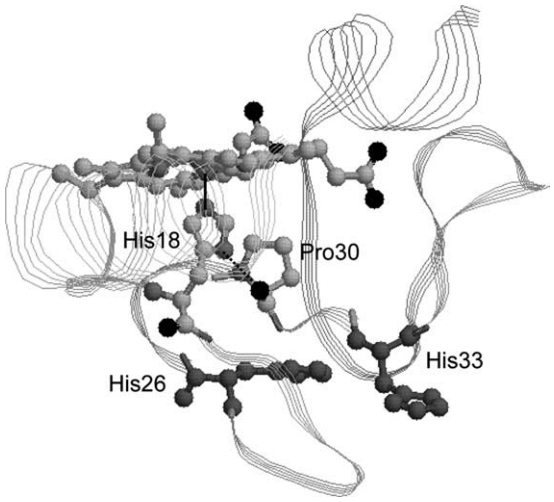


Fig. 7. Schematic representation of the 1–56 N-fragment of horse heart cytochrome *c*, based on the X-ray crystallographic structure of the native protein (PDB code 1HRC). Dotted line indicates inferred hydrogen bond, on the basis of distance criteria.

the ligand, Met80 in cyt *c* and a misligated His residue in the fragment. Moreover, protonation of methionine in cyt *c* is followed by ligation of a misligated His that, on the other hand, undergoes protonation upon further decrease of the pH. The titration of the N-fragment differs also from that of cyt *c* in the presence of denaturant agents.

At neutral pH and in the presence of GuHCl [9] or urea [26], Met80, the native axial ligand of cyt *c*, is replaced by a histidine (His33 or His26) and the protein acquires a 6cLS configuration characterized by electronic absorption and RR spectra which are indistinguishable from those of the N-fragment (Fig. 8). This form corresponds to the misligated 6cLS heme with His18 and His33 bound to the metal [26]; the same configuration is suggested for the N-fragment, which therefore may be considered a good model for the misfolded His–His intermediate formed during folding of cyt *c*. In acidic GuHCl solutions the increase of the characteristic RR HS bands at the expense of the LS bands has been clearly observed [18]. At pH 4.1 the spectral contribution of the HS configuration prevails and the spectrum resembles that of the N-fragment obtained at pH 3.0 (Fig. 2). Accordingly, the spectrum of cyt *c* in acidic GuHCl solution at pH 3.3 is very similar to that of the fragment at pH 2.0. The higher $pK_a$ for His protonation observed in the GuHCl-denatured protein ($pK_a = 5.3$) [18] with respect to the N-fragment ($pK_a = 4.15$), suggests that the 57–104 peptide segment hinders His coordination to the heme iron in the unfolded protein, likely due to steric tensions deriving from an increased protein flexibility. This is confirmed by the observation that at low ionic strength no appreciable conformational change is detected in cyt *c* (where the 57–104 segment contributes to the overall rigidity and stability of the macromolecule) in the pH range 3.8–7.0, even though a ligand (Met80) weaker than His is coordinated to the metal. Therefore we deduce that, under native-like conditions, the 57–104 peptide fragment imparts structural stability to cyt *c* by protecting the heme from the solvent accessibility.

Table 3
Scheme of the coordination-spin state changes observed for cyt *c* and the N-fragment upon lowering the pH

| **N-fragment** | | **Cyt *c*** | |
|---|---|---|---|
| **pH 7.0** | | **pH 7.0** | |
| His–Fe–His18 | 6cLS (2) | Met80–Fe–His18 | 6cLS (1) |
| **pH 5.2** | | **pH 3.8** | |
| Dissociation of the misligated His | | Dissociation of Met80 | |
| **pH 3.8** | | **pH 2.5** | |
| | | Met80–Fe–His18 | 6cLS (1) |
| His–Fe–His18 | 6cLS (2) | His–Fe–His18 | 6cLS (2) |
| $H_2O$–Fe–His18 | 6cHS (1) | $H_2O$–Fe–His18 | 6cHS (1) |
| Fe–His18 | 5cHS (1) | | |
| **pH 3.0** | | **pH 2.3** | |
| | | Met80–Fe–His18 | 6cLS (1) ↓ |
| His–Fe–His18 | 6cLS (2) ↓ | His–Fe–His18 | 6cLS (2) ↑ |
| $H_2O$–Fe–His18 | 6cHS (1) ↓ | | |
| $H_2O$–Fe–$H_2O$ | 6cHS (2) | $H_2O$–Fe–$H_2O$ | 6cHS (2) |
| Fe–His18 | 5cHS (1) ↓ | | |
| Fe–$H_2O$ | 5cHS (2) | Fe–$H_2O$ | 5cHS (2) |
| **pH 2.0** | | **pH 1.3** | |
| | | Met80–Fe–His18 | 6cLS (1) ↓ |
| His–Fe–His18 | 6cLS (2) ↓ | His–Fe–His18 | 6cLS (2) ↓ |
| $H_2O$–Fe–$H_2O$ | 6cHS (2) | $H_2O$–Fe–$H_2O$ | 6cHS (2) |
| Fe–$H_2O$ | 5cHS (2) | Fe–$H_2O$ | 5cHS (2) |

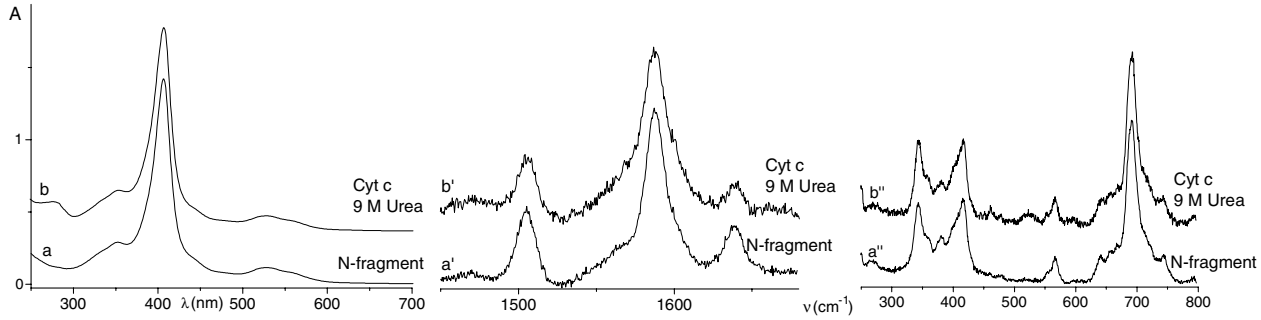


Fig. 8. Electronic absorption spectra of the oxidized N-fragment at pH 7.0 (a, a′, a″) and of cyt *c* in 9 M urea pH 7.0 (b, b′, b″). RR experimental conditions: 406.7 nm excitation wavelength; 5 $cm^{-1}$ resolution. (a′) 20 mW at the sample, 22 s/0.5 $cm^{-1}$ collection interval; (b′) 20 mW at the sample, 9 s/0.5 $cm^{-1}$ collection interval; (a″) 15 mW laser power at the sample, 3 s/0.5 $cm^{-1}$ collection interval; (b″) 20 mW at the sample, 11 s/0.5 $cm^{-1}$ collection interval.

When the protein is partially unfolded (as in the presence of GuHCl), the misligated His is more sensitive to protonation than in the N-fragment. This suggests that the lack of the (57–104 residues) segment is a stabilizing factor for the N-fragment at acid pH as the remaining peptide shields better the heme from the solvent. These considerations are in very good agreement with the redox potentials ($E_0 \simeq 250$ mV (vs NHE)) for native cyt *c*, $E_0 \simeq 10$ mV for the GuHCl-unfolded cyt *c*, $E_0 \simeq 0$ mV for the N-fragment, at neutral pH and 25 °C [16,37], that confirm the efficient shielding action of the 1–56 peptide in the N-fragment.

## 4. Conclusions

The present results provide clear evidence that the 1–56 N-fragment at neutral pH has two His residues axially coordinated to the heme iron. One is the native His18, the other is His33 (or His26) in place of (the missing) Met80. At present we cannot identify which His replaces the methionine, as both His 26 and His33 lie on the opposite side of the heme plane in native cyt *c* (Fig. 7) [20]. The fragment shows the same spectroscopic characteristics as ferric and ferrous cyt *c* under partially denaturing conditions when a non native histidine (either His26 or His33) ligand is known to replace Met80 [9]. Moreover, the misligated state of cyt *c* and the N-fragment have very similar dichroic spectra both in the Soret and in the far-UV regions [16,38–40]. Nevertheless, the peptide chain shields the heme group from solvent and the titration (as a function of pH) of the ferric fragment shows a similar behavior to the GuHCl-denatured protein albeit with lower p$K_a$.

At acidic pH one axial ligand (a His which replaces the Met residue that is coordinated at neutral pH in native cyt *c*, and a misligated His in the N-fragment and the GuHCl-denatured protein) is lost. Further, the formation of an aquo 6c HS form is observed at pH 3.8 for native cyt *c* and at pH 5.2 for the N-fragment, whereas His18 is replaced by a water molecule at pH 2.3 for cyt *c* and at pH 3.0 for the N-fragment. The latter result indicates that the peptide segment missing in the N-fragment affects the His18–Fe(III) axial bond strength, likely through a shielding action. Hence, in ferric cyt *c* the Fe–His18 bond breaks only under extreme conditions (as, for example, at very low pH or in the presence of GuHCl at pH 3.3), whereas in ferrous cyt *c* replacement of His18 is not observed even under these extreme conditions. Thus, the rupture of this bond requires extensive degradation of the overall secondary structure [18].

In the ferrous N-fragment, the misligated His has a p$K_a$ around 7.0. On the other hand, the fairly high frequency of the Fe–Im (His18) stretching mode observed in the ferrous form of the remaining 5c HS species indicates the persistence of a strong Fe(II)–Im bond even in the absence of an appropriate protein fold in the immediate environment of His18.

## 5. Abbreviations

| | |
|---|---|
| Cyt *c* | cytochrome *c* |
| GuHCl | guanidine hydrochloride |
| SDS | sodium dodecyl sulfate |
| CT1 | long wavelength (>600 nm) porphyrin (π)-to-iron ($d_\pi$) charge transfer band |
| CT | porphyrin (π)-to-iron ($d_{z^2}$) charge transfer band (695 nm), regarded as a diagnostic indicator of the integrity of the Met80–$Fe^{3+}$ bond and the native conformation of ferricytochromes *c* |
| CD | circular dichroism |
| EPR | electron paramagnetic resonance |
| RR | resonance Raman |
| 5c | five coordinate |
| 6c | six coordinate |
| HS | high spin |
| LS | low spin |

## Acknowledgements

We thank Enrica Droghetti for her assistance with curve-fitting.

This work was funded by grants from the Italian Ministry of Education, Universities, and Research (MIUR) (COFIN 2001031798).

## References

[1] Y. Goto, N. Takahashi, A.L. Fink, Biochemistry 29 (1990) 3480–3488.
[2] D. Hamada, Y. Kuroda, M. Kataoka, S. Aimoto, T. Yoshimura, Y. Goto, J. Mol. Biol. 256 (1996) 172–186.
[3] T. Jordan, J.C. Eads, T.G. Spiro, Protein Sci. 4 (1995) 716–728.
[4] C.-K. Chan, Y. Hu, S. Takahashi, D.L. Rousseau, W.A. Eaton, Proc. Natl. Acad. Sci. USA 94 (1997) 1779–1784.
[5] S.-R. Yeh, S. Han, D.L. Rousseau, Acc. Chem. Res. 31 (1998) 727–736.
[6] S.-R. Yeh, D.L. Rousseau, Nat. Struct. Biol. 5 (1998) 222–228.
[7] S.-R. Yeh, D.L. Rousseau, J. Biol. Chem. 274 (1999) 17853–17859.
[8] C. Indiani, G. De Sanctis, F. Neri, H. Santos, G. Smulevich, M. Coletta, Biochemistry 39 (2000) 8234–8242.
[9] W. Colon, L.P. Wakem, F. Sherman, H. Roder, Biochemistry 36 (1997) 12535–12541.
[10] S. Takahashi, S.-R. Yeh, T.K. Das, C.-K. Chan, D.S. Gottfried, D.L. Rousseau, Nat. Struct. Biol. 4 (1997) 44–50.
[11] G. Corradin, H.A. Harbury, Proc. Natl. Acad. Sci. USA 68 (1971) 3036–3039.
[12] G. Corradin, H.A. Harbury, Biochem. Biophys. Res. Commun. 61 (1974) 1400–1406.
[13] M. Juillerat, G.R. Parr, H. Taniuchi, J. Biol. Chem. 255 (1980) 845–853.
[14] X. Kang, J. Carey, J. Mol. Biol. 285 (1999) 463–468.
[15] A. Fontana, M. Zambonin, V. De Filippis, M. Bosco, P. Polverino de Laureto, FEBS Lett. 362 (1995) 266–270.
[16] R. Santucci, L. Fiorucci, F. Sinibaldi, F. Polizio, A. Desideri, F. Ascoli, Arch. Biochem. Biophys. 379 (2000) 331–336.
[17] F. Sinibaldi, L. Fiorucci, G. Mei, T. Ferri, A. Desideri, F. Ascoli, R. Santucci, Eur. J. Biochem. 268 (2001) 4537–4543.
[18] S. Oellerich, H. Wackerbarth, P. Hildebrandt, J. Phys. Chem. Part B (2002) 6566–6580.
[19] N.T. Yu, R.B. Srivastava, J. Raman Spectrosc. 9 (1980) 166–171.
[20] A.M. Berghuis, G.D. Brayer, J. Mol. Biol. 223 (1992) 959–976.
[21] S. Hu, I.K. Morris, J.P. Singh, K.M. Smith, T.G. Spiro, J. Am. Chem. Soc. 115 (1993) 12446–12458.
[22] J.L. Hoard, Ann. NY Acad. Sci. 206 (1973) 18–31.
[23] L.D. Spaulding, C.C. Chang, N.T. Yu, R.H. Felton, J. Am. Chem. Soc. 97 (1975) 2517–2525.
[24] S. Choi, T.G. Spiro, K.C. Langry, K.M. Smith, D.L. Budd, G.N. La Mar, J. Am. Chem. Soc. 104 (1982) 4345–4351.
[25] L.D. Sparks, K.K. Anderson, C.J. Medforth, K. Smith, J.A. Shelnutt, Inorg. Chem. 33 (1994) 2297–2302.
[26] B.S. Russell, K.L. Bren, J. Biol. Inorg. Chem. 7 (2002) 909–916.
[27] A. Boffi, T.K. Das, S. Della Longa, C. Spagnuolo, D.L. Rousseau, Biophys. J. 77 (1999) 1143–1149.
[28] T.J. Fiedler, C.A. Davey, R.E. Fenna, J. Biol. Chem. 275 (2000) 11964–11971.
[29] T.G. Spiro, X.-Y. Li, in: T.G. Spiro (Ed.), Biological Applications of Raman Spectroscopy, Wiley, New York, 1988 (Chapter 1).
[30] S.-R. Yeh, S. Takahashi, B. Fan, D.L. Rousseau, Nat. Struct. Biol. 4 (1997) 51–56.
[31] D.B. O'Connor, R.A. Goldbeck, J.H. Hazzard, D.S. Kliger, M.A. Cusanovich, Biophys. J. 65 (1993) 1718–1726.
[32] M.P. Roach, A.E. Pond, M.R. Thomas, S.G. Boxer, J.H. Dawson, J. Am. Chem. Soc. 121 (1999) 12088–12093.
[33] A.K. Bhuyan, R. Kumar, Biochemistry 41 (2002) 12821–12834.
[34] P. Stein, T.G. Spiro, J. Am. Chem. Soc. 102 (1980) 7795.
[35] H. Hori, T. Kitagawa, J. Am. Chem. Soc. 104 (1980) 376.
[36] G. Smulevich, Biospectroscopy 4 (1998) S3–S17.
[37] T. Ferri, A. Poscia, F. Ascoli, R. Santucci, Biochim. Biophys. Acta 1298 (1996) 102–108.
[38] Y.P. Myer, L.H. MacDonald, B.C. Verma, A. Pande, Biochemistry 19 (1980) 199–207.
[39] R. Santucci, M. Brunori, F. Ascoli, Biochim. Biophys. Acta 914 (1987) 185–189.
[40] Y.G. Thomas, R.A. Goldbeck, D.S. Kliger, Biopolymers (Biospectroscopy) 57 (2000) 29–36.